Insight into the Complex and Dynamic Process of Activation of Matrix Metalloproteinases

Lakshmi P. Kotra,[§,||] Jason B. Cross,[§] Yoichiro Shimura,[‡] Rafael Fridman,[‡] H. Bernhard Schlegel,[§] and Shahriar Mobashery*,[§]

Contribution from the Department of Pathology, Department of Chemistry, and Institute for Drug Design, Wayne State University, Detroit, Michigan 48202-3489

Received May 30, 2000

Abstract: Matrix metalloproteinases (MMPs) are important hydrolytic enzymes with profound physiological and pathological functions in living organisms. MMPs are produced in their inactive zymogenic forms, which are subsequently proteolytically activated in an elaborate set of events. The propeptide in the zymogen blocks the active site, with a cysteine side-chain thiolate from this propeptide achieving coordination with the catalytically important zinc ion in the active site. Molecular dynamics simulations, ab initio calculations, and wet chemistry experiments presented herein argue for the critical importance of a protonation event at the coordinated thiolate as a prerequisite for the departure of the propeptide from the active site. Furthermore, a catalytically important glutamate is shown to coordinate transiently to the active-site zinc ion to "mask" the positive potential of the zinc ion and lower the energy barrier for dissociation of the protonated cysteine side chain from the zinc ion. In addition, a subtle conformational change by the propeptide is needed in the course of zymogen activation. These elaborate processes take place in concert in the activation process of MMPs, and the insight into these processes presented herein sheds light on a highly regulated physiological process with profound consequences for eukaryotic organisms.

Proper interactions of eukaryotic cells with the extracellular matrix (ECM) are important for the normal functions within a tissue. ECM−cell interactions are regulated by a family of at least 27 zinc-dependent endopeptidases known as matrix metalloproteinases (MMPs), the functions of which have profound consequences in organ development, tissue remodeling, embriogenesis, wound healing, and angiogenesis.[1] Because of the critical functions of these enzymes in many physiological processes, their activities are strictly regulated.[2] Each is produced as an inactive zymogen form (pro-MMP), which requires activation for generation of the catalytically competent enzyme. The process of zymogen activation appears to be complicated.[3,4] A second level of control of MMP activity is exerted by inhibition of the active enzymes by a group of four specific proteins known as the tissue inhibitors of metalloproteinases ("TIMPs"). When these elaborate regulatory processes fail, the uncontrolled MMP activities contribute to the development of a variety of pathological processes including tumor metastasis, tumor angiogenesis, arthritis, connective tissue diseases, inflammation, and cardiovascular and autoimmune diseases.[5]

Depending on the type of MMP, the process of activation involves both the action of other proteases and autocatalytic events acting sequentially to remove the entire propeptide of the zymogenic form. Insights into these events are just beginning to emerge.[3,6−8] For example, the zymogenic forms of the gelatinases, pro-MMP-2 and pro-MMP-9, have propeptides of 79 and 86 amino acids, respectively. The propeptide blocks the active site, and a cysteine side-chain thiolate within the propeptide coordinates with the catalytic zinc ion (Figure 1). During activation, the propeptide in these two enzymes is hydrolyzed at the first site by another protease [for example, MMP-3 (stromelysin-1) hydrolyzes pro-MMP-9, whereas MMP-14 (MT1-MMP) does so on pro-MMP-2].[7,8] The MMP-3-mediated activation of pro-MMP-9 involves cleavage of the Glu^{40}-Met^{41} amide bond, to generate an inactive 85-kDa form, which is followed by the cleavage at the Arg^{87}-Phe^{88} bond, resulting in a fully active 82-kDa enzyme. Both sites are cleaved by MMP-3. In the case of pro-MMP-2, the first cleavage at the Asn^{66}-Leu^{67} bond is accomplished by MMP-14, which is

(1) Massova, I.; Kotra, L. P.; Fridman, R.; Mobashery, S. *FASEB J.* **1998**, *12*, 1075−1095. Forget, M.-A.; Desrosier, R. R.; Béliveau, R. *Can. J. Physiol. Pharmacol.* **1999**, *77*, 465−480. Nagase, H.; Woessner, J. F., Jr. *J. Biol. Chem.* **1999**, *274*, 21491−21494.
(2) Brew, K.; Dinakarpandian, D.; Nagase, H. *Biochim. Biophys. Acta* **2000**, *1477*, 267−283. Gomez, D. E.; Alonso, D. F.; Yoshiji, H.; Thorgeirsson, U. P. *Eur. J. Cell. Biol.* **1997**, *74*, 111−122. Birkedal-Hansen, H.; Moore, W. G.; Bodden, M. K.; Windsor, L. J.; Birkedal-Hansen, B.; DeCarlo, A.; Engler, J. A. *Crit. Rev. Oral Biol. Med.* **1993**, *4*, 197−250.
(3) Murphy, G.; Stanton, H.; Cowell, S.; Butler, G.; Knauper, V.; Atkinson, S.; Gavrilovic, J. *APMIS* **1999**, *107*, 38−44. Murphy, G.; Knauper, V.; Cowell, S.; Hembry, R.; Stanton, H.; Butler, G.; Freije, J.; Pendas, A. M.; Lopez-Otin, C. *Ann. N.Y. Acad. Sci.* **1999**, *878*, 25−39.
(4) Morgunova, E.; Tuuttile, A.; Bergmann, U.; Isupov, M.; Lindqvist, Y.; Schneider, G.; Tryggvason, K. *Science* **1999**, *284*, 1667−1669.

(5) Nelson, A. R.; Fingleton, B.; Rothenberg, M. L.; Matrisian, L. M. *J. Clin. Oncol.* **2000**, *18*, 1135−1149.
(6) Sang, Q. A.; Bodden, M. K.; Windsor, L. J. *J. Protein Chem.* **1996**, *3*, 243−253.
(7) Olson, M. W.; Bernando, M.; Pietila, M.; Gervasi, D. C.; Toth, M.; Kotra, L. P.; Massova, I.; Mobashery, S.; Fridman, R. *J. Biol. Chem.* **2000**, *275*, 2661−2668.
(8) Will, H.; Atkinson, S. J.; Butler, G. S.; Smith, B.; Murphy, G. *J. Biol. Chem.* **1996**, *271*, 17119−17123. Pei, D.; Weiss, S. J. *J. Biol. Chem.* **1996**, *271*, 9135−9140. Butler, G. S.; Butler, M. J.; Atkinson, S. J.; Will, H.; Tamura, T.; van Westrum, S. S.; Crabbe, T.; Clements, J.; d'Ortho, M.-P.; Murphy, G. *J. Biol. Chem.* **1998**, *273*, 871−880.
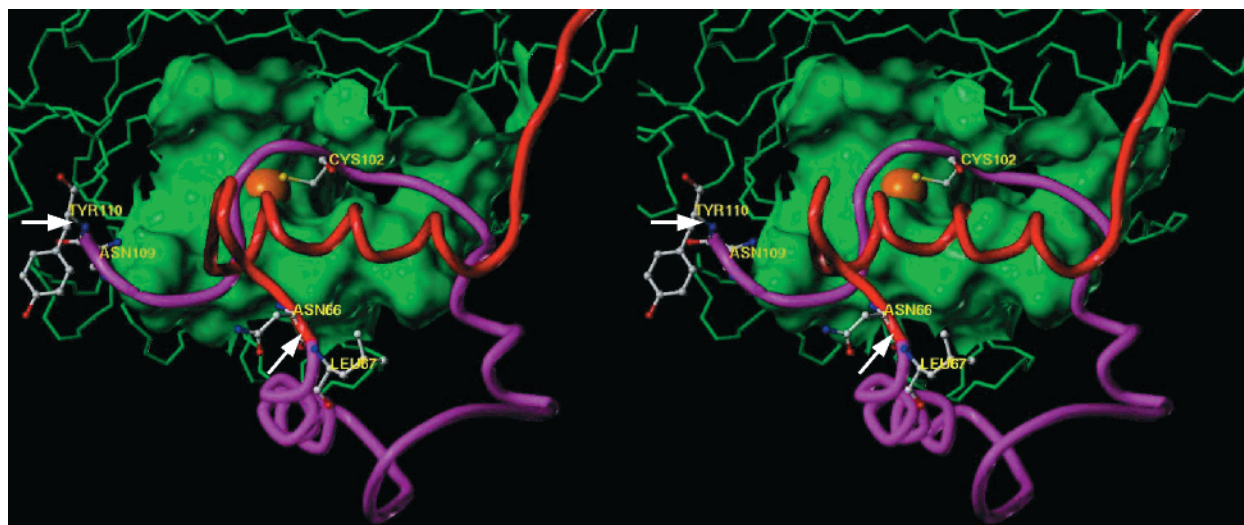
Figure 1. Stereoview of the X-ray crystal structure of proMMP-2 (1CK7). The backbone of the catalytic and gelatin-binding domains are shown in green with the active site depicted as a green surface. The catalytic zinc ion is depicted as an orange sphere, and Cys[102] is shown in ball-and-stick. The backbone of the propeptide is represented as a tube. The backbone of the propeptide region in red is released after the first hydrolytic step by stromelysin-1 at the Asn[66]-Leu[67] peptide bond (indicated by the arrow at 7 o'clock). The remainder of the propeptide, given in magenta, is released after the second hydrolytic step at the Asn[109]-Tyr[110] peptide bond (indicated by the white arrow at 9 o'clock). The side chains of residues Asn-66, Leu-67, Asn109, and Tyr 110 are shown in the ball-and-stick representation.

followed by an intermolecular autocatalytic cleavage of the Asp[109]-Tyr[110] bond, resulting in full activation. We have shown recently that the second cleavage event in pro-MMP-9 activation appears to be the rate-limiting step, and the hydrolytic activation event would appear to require a conformational motion of the propeptide.[7] We provide herein insights from computational and experimental investigations of this process, and propose for the first time the necessary incremental steps for the formation of the catalytically competent MMPs.

Methods

Computations. The X-ray coordinates of proMMP-2 were obtained from RCSB protein databank (code: 1CK7). The residue numbers are according to Swiss-Prot entry of MMP-2 sequence (COG2_HUMAN). The three-dimensional structure of pro-MMP-2 from Leu[67] (site of the first cleavage) to Pro[449], with relevant crystallographic water molecules was used and Ala[404] in the X-ray crystal structure was mutated to glutamate *in silico*. Energy minimizations and molecular dynamics simulations were performed using the Amber 5.0 suite of programs.[9] The enzyme was solvated in a periodic box of TIP3 waters of at least 10 Å thickness from the surface of the enzyme. A nonbonded cutoff of 12 Å was used, and for molecular dynamics, electrostatics were treated by the Ewald procedure as implemented in Amber 5. Molecular dynamics simulations were performed by initially equilibrating the system at constant volume for 10 ps and an additional 40 ps at constant pressure at 300 K, with time increments of 2 fs. Snapshots were collected from 5 to 250 ps for every 500 steps (1 ps). The zinc ion and the coordinated histidine nitrogens were treated as bonded atoms, and the charge of the zinc ion ($+1.62$) was calculated by partitioning the B3LYP/6-31G(d) wave function using the Merz−Singh−Kollman electrostatic potential scheme.[10] Ab initio calculations were performed

using the Gaussian 98[11] set of molecular orbital programs on a model of the active site consisting of the zinc ion, three imidazoles, ethanethiol, and a butyrate. The Zn−S bond energies were computed using the B3LYP[12] hybrid density functional with the 6-31G(d) basis set[13] (Wachters-Hay basis set[14] for Zn).

Construction, Expression and Purification of Glu[402]→Ala proMMP-9 Mutant. The following mutagenic primers were designed: 5′-GGC GGC GCA TGC GTT CGG CCA CGC GC-3′ and 5′-GCG CGT GGC CGA ACG ACT GCG CCG CC-3′ (underline indicates the mutagenized codon) to generate the Glu[402]→Ala pro-MMP-9 mutant variant using the full-length cDNA of human pro-MMP-9 cloned into the pTF7-EMCV1 expression vector as a template[15] and the Quick-Change site-directed mutagenesis kit (Stratagene). The resultant pro-MMP-9 cDNA (Glu[402]→Ala) was sequenced in both directions to confirm that the right substitution was obtained. Pro-MMP-9 Glu[402]→Ala mutant protein was expressed in nonmalignant monkey kidney epithelial BS-C-1 (CCL-26) cells using a recombinant vaccinia expression system as previously described.[16] The recombinant Glu[402]→Ala mutant was purified by gelatin affinity chromatography from the media of the infected cells as described.[15] The homogeneity of the purified proteins

(9) Case, D. A.; Pearlman, D. A.; Caldwell, J. W.; Cheatham, T. E., III; Ross, W. S.; Simmerling, C. L.; Darden, T. A.; Merz, K. M.; Stanton, R. V.; Cheng, A. L.; Vincent, J. J.; Crowley, M.; Ferguson, D. M.; Radmer, R. J.; Seibel, G. L.; Singh, U. C.; Weiner, P. K.; Kollman, P. A. *AMBER 5*; University of California: San Francisco, CA, 1997. Pearlman, D. A.; Case, D. A.; Caldwell, J. W.; Ross, W. S.; Cheatham, T. E., III; DeBolt, S.; Ferguson, D.; Seibel, G.; Kollman, P. A. *Comput. Phys. Commun.* **1995**, *91*, 1−41.

(10) Besler, B. H.; Merz, K. M., Jr.; Kollman, P. A. *J. Comput. Chem.* **1990**, *11*, 431−439. Singh, U. C.; Kollman, P. A. *J. Comput. Chem.* **1984**, *5*, 129−145

(11) Frisch, M. J.; Trucks, G. W.; Schlegel, H. B.; Scuseria, G. E.; Robb, M. A.; Cheeseman, J. R.; Zakrzewski, V. G.; Montgomery, J. A., Jr.; Stratmann, R. E.; Burant, J. C.; Dapprich, S.; Millam, J. M.; Daniels, A. D.; Kudin, K. N.; Strain, M. C.; Farkas, O.; Tomasi, J.; Barone, V.; Cossi, M.; Cammi, R.; Mennucci, B.; Pomelli, C.; Adamo, C.; Clifford, S.; Ochterski, J.; Petersson, G. A.; Ayala, P. Y.; Cui, Q.; Morokuma, K.; Malick, D. K.; Rabuck, A. D.; Raghavachari, K.; Foresman, J. B.; Cioslowski, J.; Ortiz, J. V.; Stefanov, B. B.; Liu, G.; Liashenko, A.; Piskorz, P.; Komaromi, I.; Gomperts, R.; Martin, R. L.; Fox, D. J.; Keith, T.; Al-Laham, M. A.; Peng, C. Y.; Nanayakkara, A.; Gonzalez, C.; Challacombe, M.; Gill, P. M. W.; Johnson, B. G.; Chen, W.; Wong, M. W.; Andres, J. L.; Head-Gordon, M.; Replogle, E. S.; Pople, J. A. *Gaussian 98*; Gaussian, Inc.: Pittsburgh, PA, 1998.

(12) Becke, A. D. *Phys. Rev. A* **1988**, *38*, 3098−3100; Becke, A. D. *J. Chem. Phys.* **1993**, *98*, 5648−5652; Lee, C.; Yang, W.; Parr, R. D. *Phys. Rev. B* **1988**, *37*, 785−789.

(13) Ditchfield, R.; Hehre, W. J.; Pople, J. A. *J. Chem. Phys.* **1971**, *54*, 724−728; Hariharan, P. C.; Pople, J. A. *Theor. Chim. Acta* **1973**, *28*, 213−222.

(14) Wachters, A. J. H. *J. Chem. Phys.* **1970**, *52*, 1033; Hay, J. P. *J. Chem. Phys.* **1977**, *66*, 4377; Raghavachari, K.; Trucks, G. W. *J. Chem. Phys.* **1989**, *91*, 1062.

(15) Olson, M.; Gervasi, D. C.; Mobashery, S.; Fridman, R. *J. Biol. Chem.* **1997**, *272*, 29975−29983.

(16) Fridman, R.; Fuerst, T. R.; Bird, R. E.; Hoyhtya, M.; Oelkuct, M.; Kraus, S.; Komarek, D.; Liotta, L. A.; Berman, M. L.; Stetler-Stevenson, W. G. *J. Biol. Chem.* **1992**, *267*, 15398−15405.

was monitored by SDS-polyacrylamide gel electrophoresis (SDS-PAGE). To produce ^{35}S-labeled enzymes, BS-C-1 cells were metabolically labeled with 100 μCi/ml of ^{35}S-methionine immediately after the infection−transfection procedure in Dulbecco's modified Eagle medium (DMEM, Gibco, Grand Island, NY) lacking methionine. Purification of the labeled enzymes was carried out as described above.

Activation of Wild-Type and Glu[402]→Ala proMMP-9 by Stromelysin-1. The wild-type and Glu[402]→Ala pro-MMP-9 (68 nM each) were individually incubated with activated human recombinant stromelysin-1 (6 nM) in a total volume of 300 μL of 50 mM Tris (pH 7.5), 150 mM NaCl, 5 mM CaCl$_2$, 0.02% Brij-35 (i.e., collagenase buffer). At various times, a 5 μL-portion of the mixture was added to a cuvette containing 2 mL of a 7 μM solution of the fluorescence-quenched substrate MOCAcPLGLA$_2$pr(Dnp)-AR-NH$_2$ (Peptide Institute, Inc., Japan) in 50 mM HEPES (pH 7.5) containing 150 mM NaCl, 5 mM CaCl$_2$, 0.001% Brij-35, and 1% DMSO, at 25 °C, as described previously.[15,17] Substrate hydrolysis was monitored using a Photon Technology International (PTI) fluorescence spectrophotometer with excitation and emission wavelengths set at 328 and 393 nm, respectively, controlled by a Pentium computer using the RatioMaster and Felix software provided by PTI. The excitation and emission band-passes were 1 and 3 nm, respectively.

Conversion of the wild-type and Glu[402]→Ala pro-MMP-9 to the intermediate (85 kDa) and active (82 kDa) forms by stromelysin-1 was monitored by immunoblot analysis and SDS-PAGE, followed by autoradiography of ^{35}S-labeled enzymes. The wild-type and mutant enzymes (680 nM each) were incubated at 37 °C with activated 10 nM stromelysin-1 in a total volume of 300 μL of collagenase buffer. At different times, 30 μL of the reaction mixture was collected and mixed with 10 μL of 4X SDS Laemmli sample buffer[18] without β-mercaptoethanol to stop the reaction. The samples were then subjected to nonreducing SDS-PAGE. For immunoblot analysis, the proteins were transferred to a nitrocellulose membrane, followed by detection of the antigen with the CA-209 monoclonal antibody to pro-MMP-9 recognizing both the latent and active forms.[19] Detection of the immune complexes was performed using the enhanced chemiluminescence (ECL) system (Pierce, Rockford, IL) according to the instructions of the manufacturer. For detection of the ^{35}S-labeled enzymes, the SDS-PAGE was subjected to autoradiography.

Results and Discussion

It is clear that in the activation process, coordination of the cysteine with the active-site zinc ion is lost, the hydrolytic cleavage events takes place and the propeptide is liberated from the MMP.[7,8] We investigated how the cysteine thiolate in gelatinases may be removed from the coordination sphere of the zinc ion by molecular dynamics simulations and high-level ab initio theory, using the X-ray coordinates of pro-MMP-2.[4] Preliminary analyses revealed that the critical active-site base for promotion of the hydrolytic activity, Glu[404] (corresponding to Glu[402] of pro-MMP-9), moves toward the zinc ion to achieve coordination (from 4.73 to 2.53 Å). This glutamate is conserved in all zinc proteases, and it is believed to serve the role of the general base in the "promoted-water" mechanism in these enzymes.[20] In the alternative mechanism for catalysis by zinc proteases, it has been proposed that this glutamate is involved in the formation of a mixed anhydride with the substrate, prior to hydrolysis of the intermediate.[21] Therefore, the function of
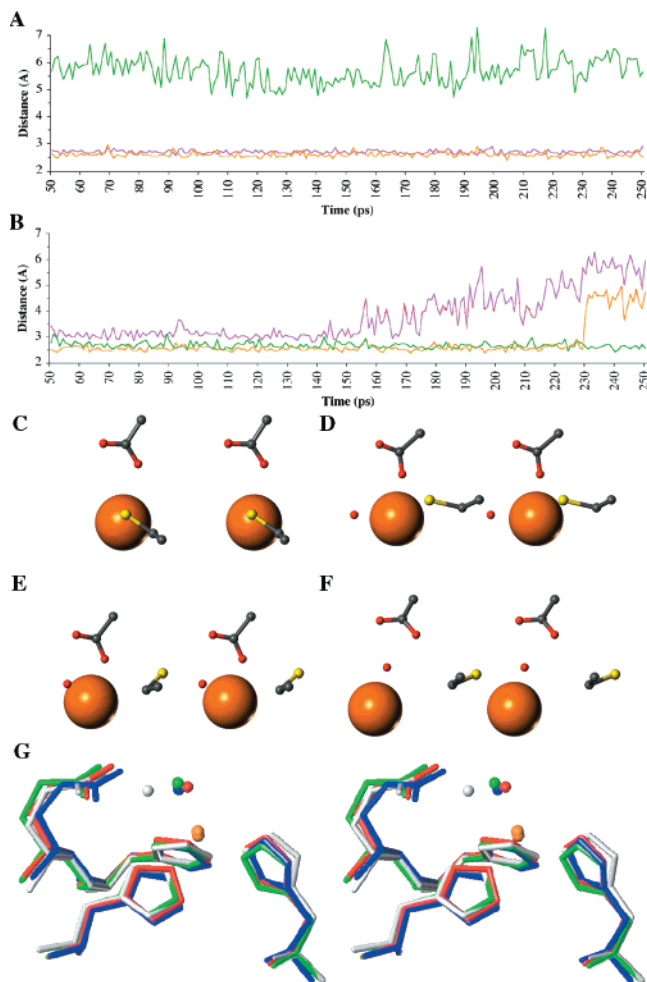
(17) Knight, C. G.; Willenbrock, F.; Murphy, G. *FEBS Lett*. **1992**, *296*, 263−266.

(18) Laemmli, U.K. *Nature* **1970**, *227*, **680**−685.

(19) Fridman, R.; Toth, M.; Peña, D.; Mobashery, S. *Cancer Res.* **1995**, *55*, 2548−2555.

(20) Christianson, D. W.; Lipscomb, W. N. *Acc. Chem. Res.* **1989**, *22*, 62

(21) Makinen, M. W.; Kuo, L.; Dymowski, J. J.; Jaffer, S. *J. Biol. Chem.*, **1979**, *254*, 356−366. Makinen, M. W.; Wells, G. B.; Kang, S. O. *Adv. Inorg. Biochem.* **1984**, *6*, 1−69. Suh, J. *Bioorg. Chem.* **1990**, *18*, 345−360.

Figure 2. Profiles of distances (Å) vs time (ps) between zinc and Cys[102] (magenta), zinc and Glu[404] (orange), and zinc and Wat[4] (green) of the molecular dynamics simulations of the pro-MMP-2 with a deprotonated Cys (A) and a protonated Cys (B) coordinating the Zn^{2+}. Stereoviews of the snapshots in the active-site region at 0 (C), 50 (D), 200 (E), and 250 ps (F). Perspectives of the active-site residues (three His, one Glu, and the zinc ion) and the hydrolytic water from the X-ray crystal structures of stromelysin-1 (blue), atrolysin C (red), and adamalysin II (green) are overlapped with those of the snapshot coordinates (gray) collected at 250 ps during the molecular dynamics simulations of MMP-2 (G). The zinc ion is shown in orange. These structures are overlapped at the following points: Cα atoms of the three His and one Glu, and the zinc ion. The RMS deviations for overlap between each of the crystal structures and the MMP-2 snapshot is less than 0.309. The spheres in blue, red, green, and gray are the water molecules from each corresponding enzyme.

this residue is indispensable for the catalytic processes of zinc proteases. The position of this glutamate is somewhat more distant from the active-site zinc ion in MMPs than in other zinc proteases of known crystal structures. The observation of the motion of the glutamate in MMP to within the coordination sphere of the zinc ion indicated to us that such coordination may reduce the bond strength between the zinc ion and the cysteine thiolate, an event that might be at the roots of the requisite rearrangement of the propeptide away from the active site. We sought to study this observation by a number of molecular dynamics simulations.

In one simulation, the metal-coordinated Cys[102] was deprotonated, and in the other it was protonated (Figure 2). We observed that Glu[404] approached zinc and coordinated with it whether Cys[102] was protonated or deprotonated (Figure 2A and 2B). However, when Cys[102] was protonated, we observed that

after Glu[404] coordination to the zinc ion, a crystallographic water molecule (Wat[4]), began to move from a starting position of 5.32 Å from the zinc ion (Figure 2C). Cys[102] thiol was at a distance of 3.09 ± 0.16 Å from zinc ion from 50 to 154 ps. From this time point on, the distance between zinc and cysteine thiol increased gradually, and reached 5.94 Å at 250 ps, accompanied by a rotation of the Cα-Cβ bond. The residue Glu[404] remained coordinated up to 229 ps. However, at 230 ps, Glu[404] shifted away from the zinc ion, while Cys[102] thiol remained at 5.42 Å from it. In the course of this time, Wat[4] had progressively approached the zinc ion (Figure 2D and 2E), and ultimately with Glu[404] moving away from the zinc ion, the water molecule achieved coordination with the active site zinc ion (2.60 Å, Figure 2F).

The final position of this water molecule is noteworthy. This type of water coordination is observed in many zinc proteases, such as stromelysin-1 (zinc—water distance 2.03 Å), atrolysin C (2.11 Å), adamalysin II (2.36 Å), neutral protease from *Bacillus cereus* DSM 3101 (1.72 Å), and serralysin (2.11 Å), among others (PDB codes: 1CQR, 1HTD, 1IAG, 1NPC, and 1SRP, respectively). Recent investigations by others on the tetrahedral coordination of Zn^{2+} over octahedral coordination in ground state using density functional theory (6−31**G-(2d, 2p)) level calculations supports our observations, where Zn^{2+} coordinates with the water molecule and three histidines in the active site (Figure 2F).[22] The snapshot from the molecular dynamics simulations at 250 ps was overlapped with the X-ray structures of stromelysin-1, atrolysin C, and adamalysin II to compare the position of the hydrolytic waters (Figure 2G). *The final spatial orientation of the water molecule coordinated with the zinc ion and the position of the active-site base (Glu[404]) are consistent with known active-site arrangements for other active zinc-dependent proteases, including MMPs; hence, we propose this to be the active species.* The propeptide is no longer coordinated to the active-site zinc ion, and the slow aforementioned structural transition (time scale of minutes) would take place,[7] and the propeptide would now be predisposed for the second proteolytic cleavage (between residues Asp[109] and Tyr[110]).

We sought to put these findings on firmer ground by investigating the Zn—S bond strength at high-level ab initio theory. Our computational active-site model (Figure 3A) consists of the zinc ion coordinated by three imidazole rings, ethanethiol (for the Cys[102] side chain), and butyrate (for the Glu[404] side chain). The spatial geometries for these residues were extracted from the X-ray structure for pro-MMP-2. The hydrogen atoms in the imidazole rings located at the positions for the Cβ of the histidines were fixed in Cartesian space to maintain the relative geometry of the active site. The Zn—N bond lengths to the imidazole rings were fixed at the crystallographic distance of 2.07 Å. The hydrogen atoms in the methyl moiety of butyrate were also fixed in Cartesian space, to mimic the protein backbone, but the flexibility of the side chain was not constrained.

In the first case, we studied the potential energy profiles of the Zn—S bond with ethanethiolate ($CH_3CH_2S^-$) to understand the bond strength of a deprotonated Cys[102] (Figure 3B). These calculations indicated that dissociation of Zn—S⁻ is reduced by 36 kcal/mol when butyrate coordinates with Zn^{2+}. It is important to note that the Zn—S⁻ bond energy remains at 105 kcal/mol, even after butyrate coordinates with Zn^{2+}. We also investigated the profiles of the potential energy of ethanethiol (representing a protonated Cys[102]) when the butyrate is in

coordination and not in coordination with Zn^{2+} (Glu-bound, and Glu-unbound, respectively) (Figure 3C). This indicated that dissociation of Zn—SH is reduced by 47 kcal/mol when butyrate carboxylate is coordinating with Zn^{2+}. The Zn—SH bond energy after butyrate coordination is 7 kcal/mol. The above observations indicate that (1) coordination of Glu[404] to Zn^{2+} may be required to "mask" the positive potential of Zn^{2+} and lower the energy-barrier for dissociation of the Zn—SH bond, and consistent with simulations, (2) protonation of Cys reduces the Zn—S bond strength substantially. The weakening of the Zn—S bond upon binding of butyrate is 11 kcal/mol greater when ethanethiol is protonated (i.e., difference of 47 and 36 kcal/mol). Thus, our ab initio calculations indicate that protonation of Cys[102] should be required prior to the dissociation of the Zn^{2+}—S coordination bond. The presence of other atoms that constitute the active site will change the energies of the species studied, however, the energetic trends noted in this study will uphold.

As discussed above, coordination of glutamate makes an important contribution toward the dissociation of the thiol from the zinc ion. We attempted to investigate this matter by expressing Glu[402]→Ala mutant variant of pro-MMP-9 (Glu[402] of pro-MMP-9 corresponds to Glu[404] of pro-MMP-2). The choice of pro-MMP-9 for this experiment was made for two reasons. First, this enzyme is fully activated by stromelysin-1 without the need of an autocatalytic event, and therefore the process of activation can be controlled. Second, pro-MMP-9 is the only MMP that to date has been shown to exhibit an equilibrium mixture of dimeric (disulfide dimer) and monomeric forms. We have recently shown that the dimeric form of pro-MMP-9 is less prone to conformational change than is the monomeric version.[7] Otherwise, the structures of the two gelatinases (MMP-2 and MMP-9) are extremely similar to one another.[23]

To investigate the role of Glu[402] in pro-MMP-9 activation, this residue was substituted by alanine. Consistent with the proposal for a critical role in catalysis for this glutamate in zinc proteases,[20,21] the mutant enzyme was devoid of activity after removal of propeptide. We investigated the ability of the purified wild-type and Glu[402]→Ala pro-MMP-9 to undergo activation by stromelysin-1. As shown in Figure 4, stromelysin-1 causes a sequential cleavage of the wild-type pro-MMP-9, resulting in the initial generation of an 85-kDa species, followed by an 82-kDa form, as previously reported.[24] The former is the product of the first proteolytic cleavage, and the latter is the fully activated MMP-9. The Glu[402]→Ala mutant exhibited an interesting property in the activation event. Whereas the monomeric form of the Glu[402]→Ala mutant showed kinetics of cleavage by stromelysin-1 that were similar to those observed with the wild-type, the dimeric mutant form, in stark contrast to the wild-type dimer, showed no detectable activation under the same conditions (Figure 4B). This result indicates that the hydrolytic cleavage did not take place with the mutant dimer.

The fact that both hydrolytic cleavages did occur for the monomeric Glu[402]→Ala mutant protein was unexpected. Analysis of the X-ray structure indicated that removal of the carboxymethyl group from Glu-402 to give the alanine variant creates a cavity that a water molecule could fill. Such a water molecule would be in the sphere of coordination with the catalytic zinc ion. The influence of this possibility was studied at the ab initio level using the previously described active site

(22) Dudev, T.; Lim; C. *J. Am. Chem. Soc.* **2000**, *122*, 11146−11153.

(23) Massova, I.; Fridman, R.; Mobashery, S. *J. Mol. Mod.* **1997**, *3*, 17− 30. Massova, I.; Kotra, L. P.; Mobashery, S. *Bioorg. Med. Chem. Lett.* **1998**, *8*, 853−858.

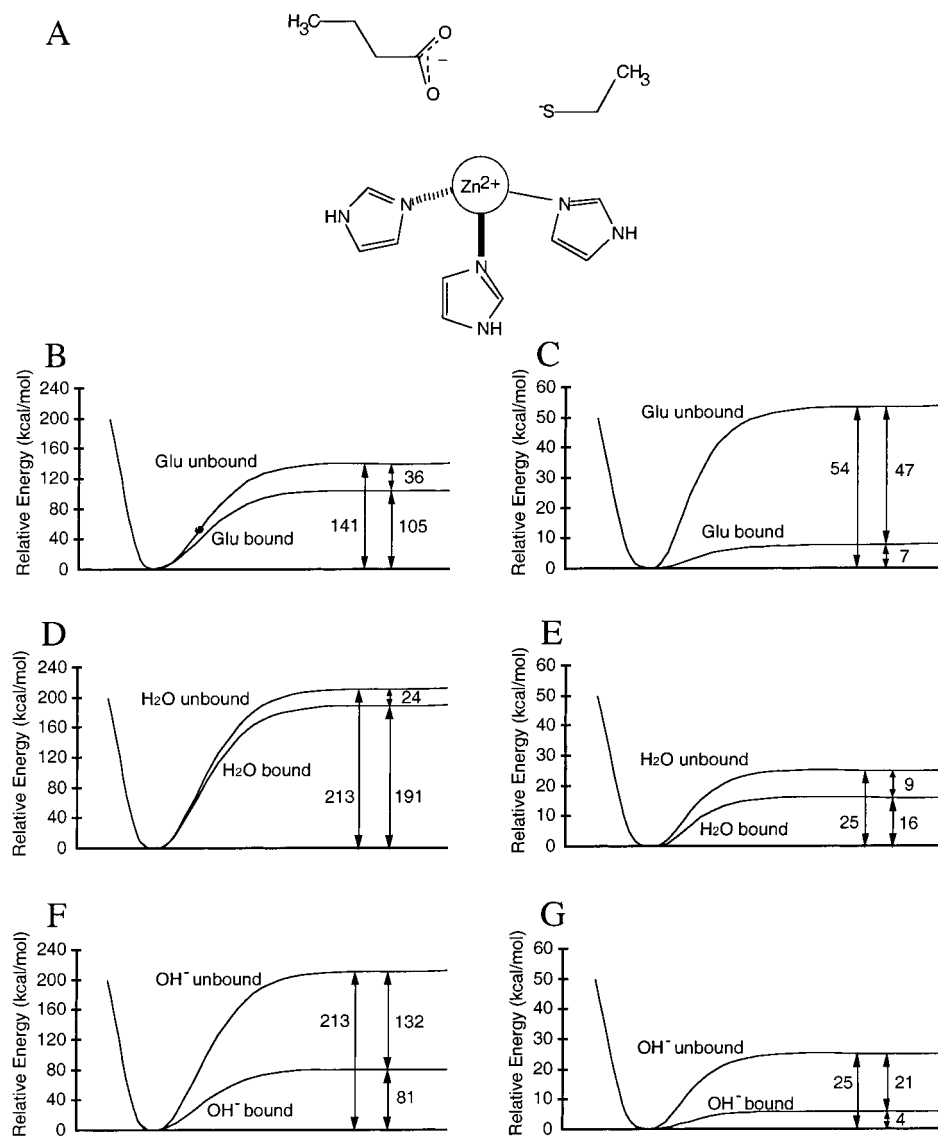(24) Ogata, Y.; Enghild, J. J.; Nagase, H. *J. Biol. Chem.* **1992**, *267*, 3581−3584.

Figure 3. Computational active-site model for ab initio calculations (A). Profiles of potential energy when ethanethiol was deprotonated (B, D, and F) and protonated (C, E, and G). Protonation reduces the $Zn-S$ bond energy by $\sim75-190$ kcal/mol depending on the species coordinated to Zn^{2+}. Binding of Glu (B and C) reduces the $Zn-S^-$ and $Zn-SH$ bond energy by 36 and 47 kcal/mol, respectively. The effect of binding water (D and E) is significantly smaller. Binding of hydroxide ion (F and G) has a very large effect on $Zn-S^-$, but a much smaller effect on $Zn-SH$ (reduction of 132 and 21 kcal/mol, respectively). It appears that dissociation of $Zn-S^-$ requires protonation of S^- and binding of a counterion to Zn^{2+}.

model modified by replacement of the coordinating carboxylate with a molecule of water or the hydroxide ion. In the case where the carboxylate is replaced by water and ethanethiolate is bound to Zn^{2+}, the $Zn-S^-$ dissociation energy is reduced by 24 kcal/mol when water coordinates to Zn^{2+}, but the dissociation energy remains at 191 kcal/mol (Figure 3D). The dissociation of $Zn-SH$, where ethanethiol is used to represent protonated Cys, is reduced by 9 kcal/mol on coordination of water to Zn^{2+}; however, the dissociation energy in this case is only 16 kcal/mol (Figure 3E). The calculations on the active site with hydroxide ion replacing the carboxylate show a more pronounced reduction in dissociation energy compared to that with replacement by water. In this case, the dissociation of ethanethiolate ($Zn-S^-$ bond) is reduced by 132 kcal/mol on coordination of hydroxide ion to Zn^{2+}, with the dissociation energy remaining at 81 kcal/mol (Figure 3F). This represents a large reduction in dissociation (110 kcal/mol) by changing the coordinating ligand from a water molecule to a hydroxide ion. The dissociation of ethanethiol ($Zn-SH$ bond) is reduced by 21 kcal/mol with

hydroxide coordinated to Zn^{2+}, resulting in a dissociation energy of 4 kcal/mol (Figure 3G). Although this is only a 12 kcal/mol reduction of the dissociation energy by changing from coordination of water to hydroxide, the dissociation energy calculated with hydroxide ion is very close to that calculated using carboxylate to represent Glu. Hence, a hydoxide ion may effectively substitute for the function of the glutamate in lowering the energy barrier for displacement of the protonated cysteine from the active site zinc ion. We believe that this is the operative process for the stromelysin-1-mediated activation of the monomeric Glu[402]→Ala pro-MMP-9.

We had argued previously that the hydrolytic cleavages in the propeptide of MMPs require a subtle but indispensable relaxation of the structure of the propeptide to make the cleavage sites available to the activating protease, since these sites are not accessible.[7] Indeed, it is a general feature of catalysis by proteases that requires a lack of secondary structure in their substrates, and for the cleavage sites in pro-MMPs to be made available for proteolysis, the secondary structures around both
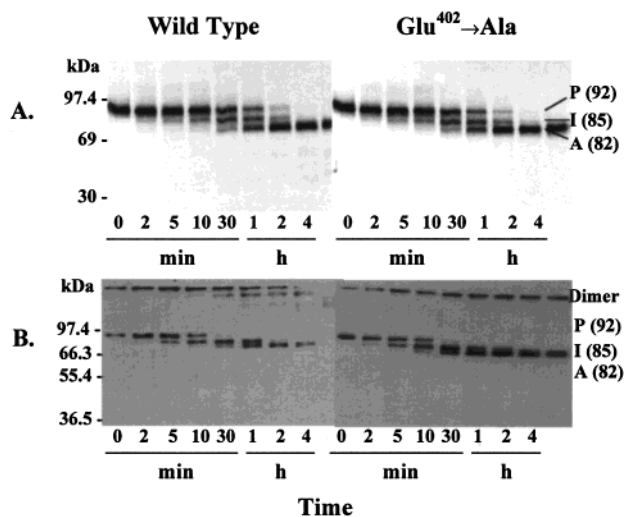
Figure 4. Purified wild-type and Glu[402]→Ala pro-MMP-9 (680 nM) were incubated at 37 °C for various times (0−240 min) with 10 nM of activated stromelysin-1. At each incubation time, an aliquot of the sample was subjected to SDS-PAGE, followed by autoradiography, reducing conditions (A) or by immunoblot analysis, nonreducing conditions (B). "P" represents the zymogenic pro-MMP-9, and "I" and "A" denote the intermediate form (∼85 kDa) and the fully active (∼82 kDa) enzymes, respectively. Note that dimeric form of pro-MMP-9 is only seen under the nonreducing conditions of panel B.

sites (Figure 1) should be relaxed. We had shown that the dimeric pro-MMP-9 form was considerably more stable, indicative of the fact that dimerization of the protein stabilized the local structure of the propeptide.[7] Structural information on the nature of the pro-MMP-9 dimer is presently lacking. Therefore, we felt that the dimeric form of pro-MMP-9 presented an opportunity to investigate the importance of the subtle conformational change for the activation event by stromelysin-1. It is quite interesting to note that the hydrolytic cleavages in the dimeric pro-MMP-9 mutant variant do not take place (Figure 4B).

These data collectively indicate that the process of zymogen activation for MMPs is substantially more complex than previously appreciated. It would appear that the necessary events for this crucial process are: (1) protonation of the cysteine thiol, which reduces the Zn−S bond strength substantially, and consistent with dynamics simulations, (2) coordination of Glu[404] to Zn^{2+} should be required to "mask" the positive potential of Zn^{2+} and lower the energy-barrier for dissociation of the Zn−SH bond. In principle, nature takes advantage of the availability of the active-site glutamate for the catalytic needs of the enzyme to facilitate the process of zymogen activation, an event that would have entropic advantage. (3) In the absence of the requisite subtle conformational change of the propeptide, the proteolytic activation does not take place.

The X-ray structures for MMPs do not present an obvious route for the travel of the proton to the coordinated zinc. No doubt that protein dynamics would play a role in bringing the proton in to facilitate the process of activation.

The findings reported herein argue for a dynamic process for activation of pro-MMPs. These sets of events are shared by all MMPs, but similar processes would be expected of other proteins, as we begin to appreciate their dynamic natures.